CHEMISTRY
A EUROPEAN JOURNAL

DOI: 10.1002/chem.200501545

The Bingel Monoadducts of La@C_{82}: Synthesis, Characterization, and Electrochemistry

Lai Feng,[a] Takatsugu Wakahara,[a] Tsukasa Nakahodo,[a] Takahiro Tsuchiya,[a] Qiuyue Piao,[a] Yutaka Maeda,[b] Yongfu Lian,[a] Takeshi Akasaka,*[a] Ernst Horn,*[c] Kenji Yoza,[d] Tatsuhisa Kato,[e] Naomi Mizorogi,[f] and Shigeru Nagase*[f]

Abstract: The reaction of La@C_{82} with diethyl bromomalonate in the presence of base (the Bingel reaction) generated five monoadducts which have been fully characterized. It was found that four of them (mono-A, -B, -C, and -D) are ESR-inactive, suggesting singly bonded regioisomers. In contrast, the fifth product (mono-E) is ESR-active, indicating that it possesses a cyclic moiety between the appended malonate group and the fullerene cage, analogous to conventional Bingel adducts. The differences in the molecular structures of mono-A, -B, -C, and -E result in varying thermal stabilities and electrochemical behavior. In particular, the singly bonded monoadducts undergo the retro-Bingel reaction either under thermal treatment or during electron transfer on the cyclic voltammetric timescale. However, mono-E shows remarkable thermal stability and perfect reversibility under the same experimental conditions.

Keywords: cycloaddition · electrochemistry · endohedral metallofullerenes · regioselectivity · structure elucidation

Introduction

Since Smalley and co-workers confirmed the existence of La@C_{82} in 1991,[1] endohedral metallofullerenes (EMFs) have attracted intense interest as a result of their unique structures and properties.[2] As a novel hybrid material of metals and fullerenes, EMFs are expected to have a wide range of potential applications in chemistry, physics, biomedicine, and nanomaterials science.[2,3] The chemistry of EMFs has recently received much attention and a variety of fullerene-related reactions have been applied to EMFs.[4–7] It has been found that the reactivities of EMFs are quite different to those of empty fullerenes. In particular, several monoadditions to EMFs have been revealed to occur with remarkable regioselectivity and to afford only a few or even only one regioisomer.[4,5b,c,6] The selectivity of these addition reactions has been ascribed to the encapsulated metal atoms or clusters which influence the electronic structure and reactivity of the fullerene cage by electron transfer. The electrochemical behavior of EMF derivatives has also been studied. Exterior modifications have been demonstrated to be a useful way of tuning the electronic properties of fullerene cores.[6a,7c] These efforts have made it possible to prepare specific fullerene materials with desired properties by internal doping with metal atoms and by exterior modification of the fullerene cage.

We have a particular interest in the Bingel reaction, which is one of the most widely applied reactions in fullerene chemistry. The first attractive Bingel adduct of EMFs to be obtained was Gd@C_{60}[$C(COOC_2H_5)$]$_n$ (n=1–10) report-

[a] Dr. L. Feng, Dr. T. Wakahara, Dr. T. Nakahodo, Dr. T. Tsuchiya, Q. Piao, Dr. Y. Lian, Prof. Dr. T. Akasaka
Center for Tsukuba Advanced Research Alliance
University of Tsukuba, Tsukuba, Ibaraki 305-8577 (Japan)
Fax: (+81) 29-853-6409
E-mail: akasaka@tara.tsukuba.ac.jp

[b] Dr. Y. Maeda
Department of Chemistry, Tokyo Gakugei University, Koganei, Tokyo 184-5801 (Japan)

[c] Prof. Dr. E. Horn
Department of Chemistry, Rikkyo University, Tokyo 171-8501(Japan)
Fax: (+81) 5992-3434
E-mail: ehorn_chem@grp.rikkyo.ne.jp

[d] Dr. K. Yoza
Bruker AXS K.K., Yokohama 221-0022 (Japan)

[e] Prof. Dr. T. Kato
Josai University, Sakado 350-0295 (Japan)

[f] Dr. N. Mizorogi, Prof. Dr. S. Nagase
Institute for Molecular Science, Okazaki 444-8585 (Japan)
Fax: (+81) 564-53-4660
E-mail: nagase@ims.ac.jp

Supporting information for this article is available on the WWW under http://www.chemeurj.org/ or from the author.

ed by TDA researchers.[8] Its hydroxylated derivative (Gd@C_{60}[C(COOH)]$_n$, $n=1$–10) has been proved to have favorable properties as a magnetic resonance imaging (MRI) contrast reagent.[3a,8] More recently, another Bingel adduct of an EMF ($Y_3N@C_{80}$) was reported. As suggested by related NMR spectroscopic analyses, a malonate group has been attached to a specific [6,6] double bond of a C_{80} cage with excellent regioselectivity.[5c] However, when we performed the Bingel reaction on La@C_{82}, its product distribution was found to be very different to those of empty fullerenes as well as previously reported EMFs.[5c,8]

Herein we describe all the monoadducts formed in this unconventional Bingel reaction of La@C_{82}. Their possible structure assignments are discussed according to not only experimental characterizations but also theoretical calculations. In addition, their stabilities and electrochemical behavior have been studied and compared with those of the parent La@C_{82}.

Results and Discussion

Synthesis and isolation: The reaction of fullerenes with diethyl bromomalonate in the presence of 1,8-diazabicyclo-[5.4.0]undec-7-ene (DBU) has been widely used to add malonate groups across the [6,6] double bonds of fullerene cages.[9] However, the use of DBU in the reaction of metallofullerenes is inadvisable because charge transfer may occur between them, similarly to the interaction between metallofullerenes and some basic nitrogen solvents such as pyridine, aniline and dimethylformamide.[10] To explore the reactivity of DBU towards La@C_{82}, we added DBU dropwise to a solution of La@C_{82} in toluene whilst stirring, which led to the formation of a precipitate in a short time. This precipitate is soluble in a mixture of CS_2 and acetone and exhibits similar absorption characteristics to $[La@C_{82}]^-TBA^+$ (TBA = tetrabutylammonium) obtained by electrolysis.[11] This result suggests that $[La@C_{82}]^-$ is formed by charge transfer from DBU to La@C_{82}. Thus, DBU actually causes the generation of a side product ($[La@C_{82}]^-$), and prevention of an excess formation of $[La@C_{82}]^-$ has to be taken into account in the Bingel reaction of La@C_{82}. We first modified the established protocol by reducing the amount of DBU used in the reaction. For instance, in a typical reaction, DBU (0.54 equiv) was added dropwise to a mixture of La@C_{82} (1 equiv) and diethyl bromomalonate (1.8 equiv). The total yield of Bingel adducts was about 25% based on the pristine La@C_{82}. The unwanted $[La@C_{82}]^-$ was formed in a yield of 4–7% and then recovered as La@C_{82} by controlled-potential electrolysis (CPE). In fact, no more than one equivalent of DBU is advisable for this reaction as excess base would otherwise lead to a dramatic increase in the formation of $[La@C_{82}]^-$, which is not wanted in the Bingel reaction of La@C_{82}.

Monoadducts were revealed to be the major products of this reaction. They were isolated from the reaction mixture by multistage high-performance liquid chromatography (HPLC). The separation scheme is shown in Figure 1. In the first stage (Figure 1a), the soluble reaction mixture was injected into a 5PYE column and a mixture of monoadducts (fraction a1 (Fra1)) was separated from the multiadducts and unreacted starting materials. Figure 1b shows the chromatogram of the second stage of the product separation, which was performed on a Buckyprep M column. Mono-E was isolated from the other monoadducts (fraction b1 (Frb1)) as a result of its longer retention time. Then, in the third stage (Figure 1c), fraction b1 obtained in the second stage was recycled on a 5PBB column. Mono-A and fraction c2 were completely separated in the second cycle. In the fourth stage (Figure 1d), mono-C was isolated from fraction d2 (mono-B and -D) by recycling fraction c2 on a Buckyprep column. However, owing to their very similar retention times, attempts to separate mono-B and -D failed on all available columns using toluene as the eluent. In the fifth stage (Figure 1e), a little better isolation was achieved by using a mixture of toluene and hexane (3:1) as the eluent on a Buckyclutcher column. Under this condition, mono-D was eluted on the front shoulder of mono-B and could be removed with the loss of some of mono-B. Therefore, mono-A, -B, -C, and -E were successfully purified. The HPLC profiles of the purified samples on different columns are shown in the Supporting Information. The product distribution was estimated to be approximately 55.4% mono-A, 22.1% mono-B, 5.1% mono-C, 5.5% mono-D, and 11.9% mono-E according to the analyses of their HPLC profiles.

Product characterizations: First, the magnetic properties of mono-A, -B, -C, -D, and -E were studied by ESR spectroscopy. The results are completely unexpected: Mono-A, -B, -C, and -D were found to be ESR-inactive, whereas mono-E was the only ESR-active species. As Figure 2 shows, the parameters of the ESR signal from mono-E, including the g value ($g=2.0019$), the hyperfine coupling constant (hfc = 1.173 G), and the peak-to-peak linewidths ($\Delta H_{pp}=0.558$ G), are similar to those of the parent La@C_{82} ($g=2.0011$, hfc = 1.152 G, $\Delta H_{pp}=0.360$ G). This suggests that mono-E retains the paramagnetic properties of the parent EMF and might be a cycloadduct of La@C_{82}. However, the other monoadducts are believed to have completely different structures.

The absolute structure of mono-A was clearly established by an X-ray crystallographic analysis performed at 93 K.[12] As shown in Figure 3, its unique structural feature is the single-bond between the appended bromomalonate group and the fullerene cage. As a result, only one electron is diverted away from the 85 π-electron system of La@C_{82}. This gives rise to a closed-shell structure of mono-A, which is in good agreement with the results of ESR spectroscopy. The addition site is far from the lanthanum atom and is located at an apex of two six-membered rings and a five-membered ring. To the best of our knowledge, this is the first definite example of a derivative of M@C_{2n} with the addition site far from the encapsulated metal atom.

Efforts to obtain single crystals of the other monoadducts have so far been unsuccessful because of their small

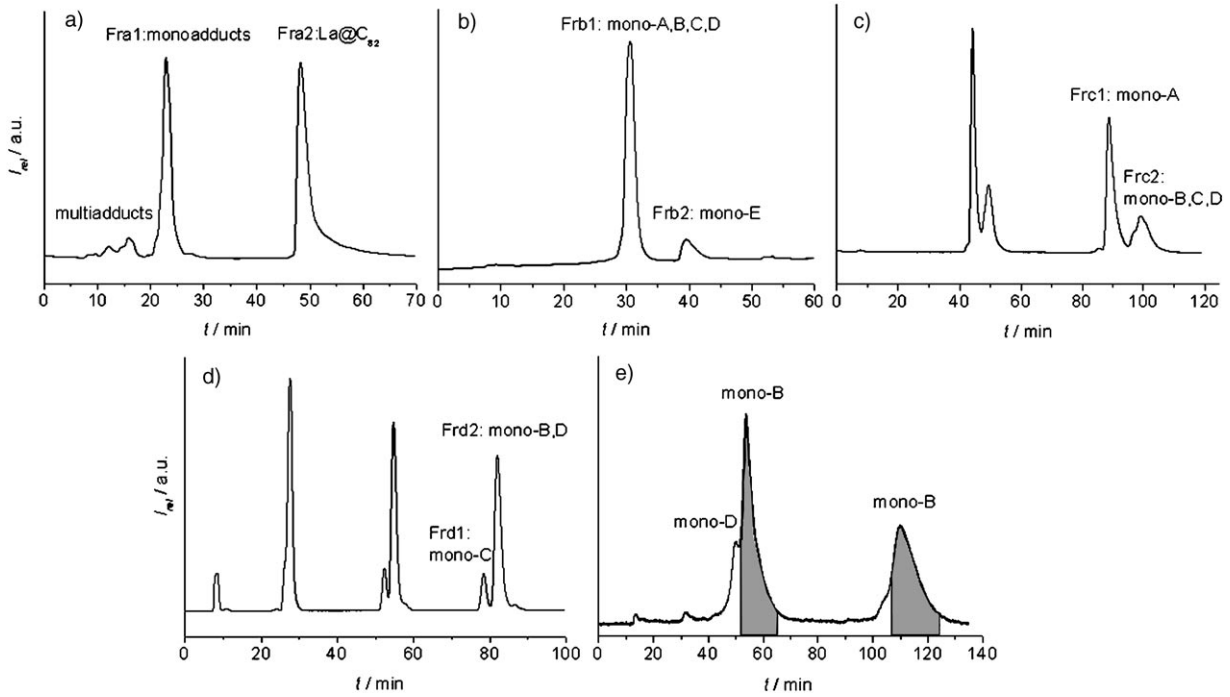

Figure 1. HPLC separation/isolation scheme for the Bingel monoadducts of La@C_{82}. a) First-stage HPLC chromatogram on a 5PYE column (Nacalai Cosmosil 20×250 mm, toluene as eluent, 9.0 mL min^{-1} flow rate); b) second-stage HPLC chromatogram on a Buckyprep M column (Nacalai Cosmosil 20×250 mm, toluene as eluent, 9.9 mL min^{-1} flow rate); c) third-stage HPLC chromatogram on a 5PBB column (Nacalai Cosmosil 20×250 mm, toluene as eluent, 9.9 mL min^{-1} flow rate); d) fourth-stage HPLC chromatogram on a Buckyprep column (Nacalai Cosmosil 20×250 mm, toluene as eluent, 9.0 mL min^{-1} flow rate); e) fifth-stage HPLC chromatogram on a Buckyclutcher column [Nacalai Cosmosil 21×500 mm, toluene and hexane (3:1) as eluent, 9.9 mL min^{-1} flow rate].

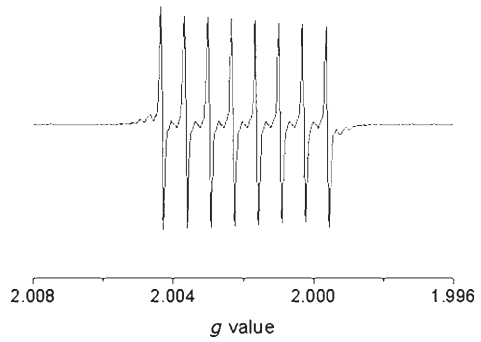

Figure 2. ESR spectrum of isolated mono-E.

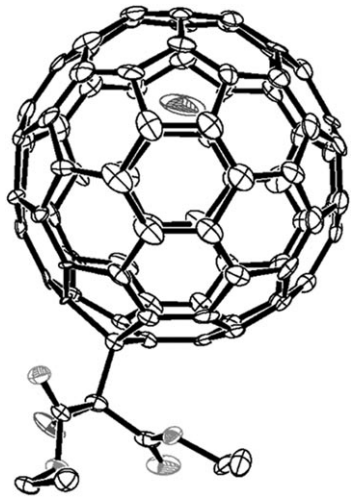

Figure 3. ORTEP drawing of mono-A (major enantiomer). Hydrogen atoms and CS_2 molecules have been omitted for clarity.

amounts. However, the NMR spectra of mono-B, -C, and -D were found to exhibit features comparable to those of mono-A. In detail, only two sets of signals due to the two ethoxy groups appear in their ^{1}H NMR spectra. In the ^{13}C NMR spectra, mono-A, -B, -C, and -D exhibit resonances from 81 carbon atoms in the range typical of sp^2 carbon atoms ($\delta = 180$–125 ppm), indicating the diversion of one sp^2 carbon atom and the C_1 symmetry of the C_{82} cage. The other signals can be assigned to the two ethoxycarbonyl groups and the C–C bond between the malonate functional group and the fullerene cage (see the Supporting Information for the NMR spectra).

Thus, NMR spectroscopic analyses suggest that mono-A, -B, -C, and -D might be regioisomers of a singly bonded monoadduct.

The paramagnetic nature of mono-E does not allow direct NMR analysis, so the anion of mono-E was prepared by the bulk electrolysis method. The ^{1}H NMR spectrum of [mono-

E]$^-$ is similar to those of mono-A, B, C, and D, with two sets of signals due to the two ethoxy groups being observed. However, [mono-E]$^-$ exhibits a different ^{13}C NMR spectrum (Figure 4): 82 sp^2 carbon atoms could be identified between

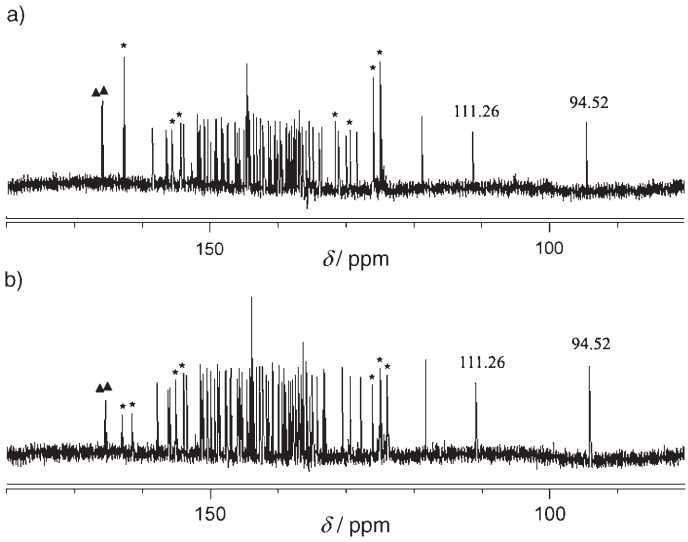

Figure 4. ^{13}C NMR of [mono-E]$^-$ a) with ^{1}H decoupling, b) without ^{1}H decoupling. The signals marked by ▲ are due to the carbonyl carbon atoms of the malonate functional group. The signals marked by * are due to impurities.

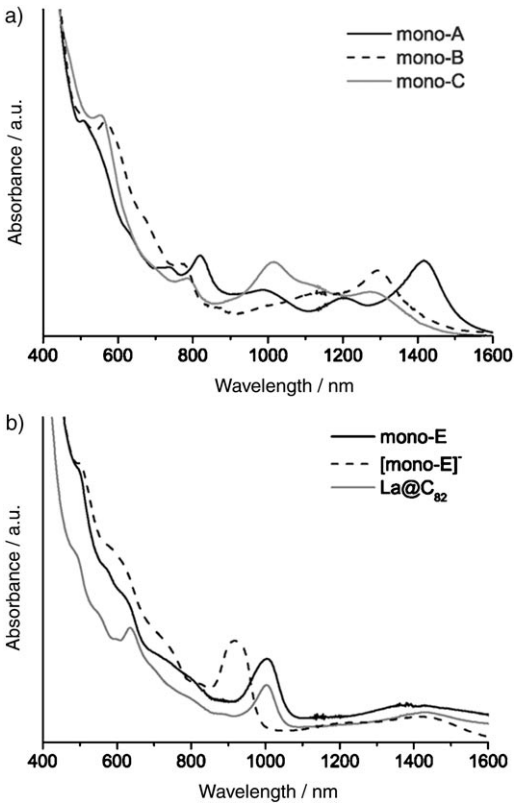

Figure 5. UV/Vis/NIR spectra of a) mono-A, -B, and -C, and b) mono-E in toluene and its anion in *o*-dichlorobenzene. The absorption profile of La@C_{82} is given as a reference.

90 and 160 ppm, corresponding to the conjugated C_{82} cage, which undoubtedly suggests that [mono-E]$^-$ also possesses C_1 symmetry. Notably, there are two carbon atoms ($\delta =$ 111.26 and 94.52 ppm) shifted upfield relative to the other 80 standard sp^2 carbon atoms. This feature is comparable to that of the ^{13}C NMR spectrum of [La@C_{82}(Ad)]$^-$ in which the two higher-field sp^2 carbon atoms ($\delta = 80$–100 ppm) have been assigned to the fullerenyl carbon atoms at [6,6] positions at which the ′open′ cycloaddition occurs.[6c] Therefore, it is reasonable to presume that one bond in the [mono-E]$^-$ cage has been opened as a result of cycloaddition of the malonate group. Since all of the 82 carbon atoms are still conjugated to each other after open cycloaddition, the electronic structure of mono-E is expected to be almost unaltered compared with the parent La@C_{82}.

Figure 5 shows the UV/Vis/NIR absorption spectra of mono-A, -B, -C, and -E, as well as of the anion of mono-E. Mono-A, -B, and -C have clearly lost most of the absorption features of the parent La@C_{82}. Their most characteristic near-IR bands are observed at 1416, 1294, and 1014 nm, respectively. Since mono-A, -B, and -C are regioisomers, their absorption spectra in the near-IR field are believed to be independent of the nature of the addend and can be distinguished by their different addition sites. All their absorption onsets move to a shorter wavelength (ca. 1600 nm), indicating larger HOMO–LUMO energy gaps. In contrast, the absorption features of mono-E are almost identical to those of La@C_{82} in the near-IR field. This suggests that mono-E retains the essential electronic structural characteristics of La@C_{82}, as predicted by NMR spectroscopy. When mono-E was reduced to [mono-E]$^-$, its color changed from brown to a little darker brown. [Mono-E]$^-$ has an absorption onset at around 1600 nm, as well as a diagnostic band at 918 nm and a broad band at 1420 nm in the near-IR field.

The MALDI-TOF mass spectra of mono-A, -B, -C, and -E are presented in the Supporting Information. Mono-A, -B, and -C exhibit similar mass spectra in either the positive or the negative mode: The most distinct peak at *m*/*z* 1123 is that of the parent La@C_{82}, while the weak peak at *m*/*z* 1281 arises from the loss of a bromine atom. No molecular-ion peak was observed for the monoadducts. In the case of mono-E, its molecular-ion peak (*m*/*z* 1281) is the most intense one in either the positive- or negative-mode mass spectrum, indicating that [mono-E]$^+$ and [mono-E]$^-$ are not so fragile as to be cleaved under the applied laser desorption conditions.

Theoretical prediction of addition sites: The theoretical calculations of the Mulliken charge densities of La@C_{82} performed at the B3LYP level of theory have revealed that C23 (the addition site in mono-A) is the most positively charged carbon atom,[12a] even though La@C_{82} has a negatively charged fullerene cage due to the three-electron donation from the encapsulated lanthanum atom.[13] Also, besides

C23, there are three other positively charged carbon atoms (C18, C21, and C14) in La@C_{82} (see Figure 6 and Table 1). Their charge densities decrease in the following order:

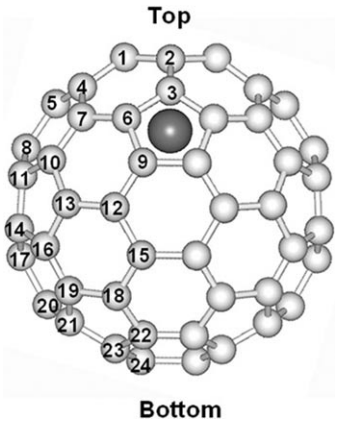

Figure 6. Schematic drawing of La@C_{82}.

Table 1. Charge densities and POAV values of the positively charged carbon atoms in La@C_{82}.

Carbon number	Charge density	POAV value
23	0.006	10.74
18	0.004	11.01
21	0.002	10.50
14	0.000	11.00

C18 > C21 > C14. On the other hand, the p-orbital axis vector (POAV) of carbon atoms is usually used as an index of local strain.[14] According to the results of the calculations, the POAV of C23 is less than that of C18. However, because of the dominant yield of mono-A, C23 appears to be the most reactive carbon atom for this Bingel reaction. The positive charge density might be more important than the local strain in the Bingel reaction of La@C_{82}. Accordingly, the addition site for the second most abundant monoadduct (mono-B) can be assigned to C18, while mono-C and -D might have addition sites at C14 and C21 (or C21 and C14), respectively.

Generally, these positively charged carbon atoms are located near the bottom of the C_{82} cage and far from the lanthanum atom. Nucleophilic addition reactions, such as the Bingel reaction, prefer to occur in this region. The highly negative charges are mainly delocalized over the top of C_{82} cage and close to the lanthanum atom. Correspondingly, electrophilic addition reactions, such as the carbene reaction, have been proved to take place at the top of the C_{82} cage.[6a,c] Therefore, the patterns of addition to La@C_{82} are expected to be selectively controlled by the type of reaction.

Thermal stabilities and electrochemical properties: Since the Bingel reaction of La@C_{82} took place at room temperature, product distribution is believed to be kinetically controlled; the reaction probably affords kinetically favored products rather than thermodynamically stable ones. To experimentally probe their thermal stabilities, mono-A, -B, -C, -D, and -E were heated in anhydrous *o*-dichlorobenzene for 6 h at 80 °C. Then the treated samples were analyzed by HPLC. Surprisingly, mono-A, -B, -C, and -D were found to decompose to give the parent La@C_{82} as the major product. These results suggest that these singly bonded monoadducts have very low thermal stabilities even though they exhibit high stabilities at low or room temperature. In contrast, mono-E showed comparatively higher stability and remained almost intact after thermal treatment.

The electrochemical properties of mono-A, -B, -C, and -E were investigated by differential pulse voltammetry (DPV) in *o*-dichlorobenzene (Figure 7). Their redox potentials obtained by DPV are listed in Table 2, together with the redox

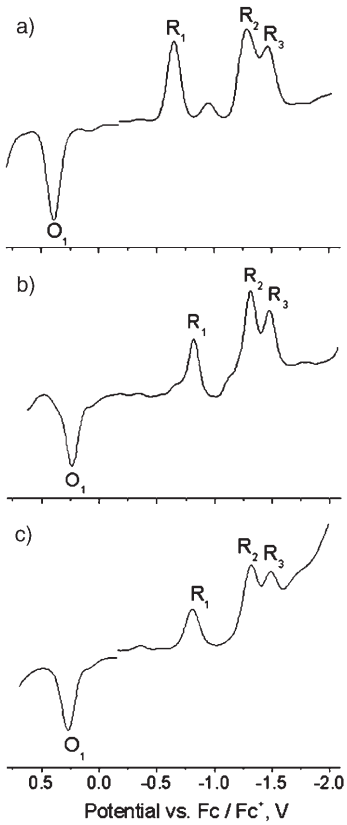

Figure 7. Differential pulse voltammograms of a) mono-A, b) mono-B, and c) mono-C in *o*-dichlorobenzene (0.1 M $(n\mathrm{Bu})_4\mathrm{NPF}_6$, 20 mV s^{-1} scan rate).

potentials of La@C_{82}[15] and its carbene derivative La@C_{82}(Ad).[6a] Because of their similar structural characters, mono-A, -B, and -C showed similar redox behavior. As Figure 7 shows, these three isomers exhibit three reduction waves and one oxidation wave in the range of 0.8 to −2.0 V. Their first oxidation waves are shifted anodically by 0.16–0.31 V relative to the value of E_1^{ox} for La@C_{82}, while their reduction waves are shifted cathodically by 0.24–0.41 V relative to the value of E_1^{red} for La@C_{82}. Although their specific

Table 2. Redox potentials[a,b] of the Bingel monoadducts of La@C_{82}.

	E_1^{ox}	E_1^{red}	E_2^{red}	E_3^{red}
mono-A	0.38	−0.66	−1.31	−1.47
mono-B	0.23	−0.83	−1.32	−1.48
mono-C	0.26	−0.82	−1.33	−1.50
mono-E	0.08	−0.28	−1.19	
La@C_{82}(Ad)[c]	−0.01	−0.49	−1.44	−1.79
La@C_{82}[c]	0.07	−0.42	−1.37	−1.53

[a] Values are in given in volts relative to a ferrocene/ferrocenium redox couple and were obtained by DPV. [b] Conditions: working electrode: platinum disk (1 mm diameter); counter-electrode: platinum wire; reference electrode: saturated calomel reference electrode (SCE); supporting electrolyte: 0.1 M (nBu)$_4$NPF$_6$ in o-dichlorobenzene. CV: scan rate, 50 mV s^{-1}. DPV: pulse amplitude, 50 mV; scan rate, 20 mV s^{-1}. [c] The redox potentials of La@C_{82} and La@C_{82}(Ad) are given for reference.

redox potentials are different, mono-A, -B, and -C have essentially identical potential gaps between their first oxidation and reduction waves (1.04, 1.06, and 1.08 V, respectively) which are much larger than that for La@C_{82} (0.49 V). This also suggests that these singly bonded monoadducts possess larger HOMO–LUMO energy gaps due to their higher-lying LUMO levels and lower-lying HOMO levels, as compared with those of La@C_{82}. Therefore, singly bonded addition dramatically modifies the electronic structure of the fullerene core with respect to the pristine one. Moreover, the first oxidation and reduction potentials of mono-A are shifted to a more positive potential than those of mono-B and -C, indicating the influence of regioisomerism. Such differences in the electrochemical behavior of regioisomers have also been reported for silylated C_{76} and C_{84}.[16]

Further studies on the electrochemical behavior of these monoadducts focused on cyclic voltammetry (CV) measurements. For mono-A, -B, and -C, each redox wave was studied independently in their potential scale. The first oxidation waves, as well as the second and third reduction waves, were found to be reversible. The first reduction waves are irreversible, even when the scan rate was increased up to 100 mV s^{-1}, indicating that [M]$^-$ [M = La@C_{82}CBr(COOC$_2$H$_5$)$_2$] is quite unstable, even on the CV timescale. In particular, as Figure 8 shows, when potentials are cathodically scanned beyond R_1, a new oxidation wave A_0 appears in the following anodic scan. This new oxidation is clearly reversible, as shown by the third segment of scans, giving rise to a reduction wave A_0' that is much more positive than the adduct-based first reduction wave R_1. Moreover, in the third or even further redox scans, R_1 exhibits a lower current, whereas A_0 and A_0' show an increased current. The $E_{1/2}$ value (ca. −0.38 V) for this new redox couple (A_0 and A_0') is close to the first reduction potential (−0.42 V) of pristine La@C_{82}. These results suggest that the first reduction of these monoadducts is followed by some rapid chemical reaction (by the EC mechanism)[17] to generate La@C_{82} (the retro-Bingel reaction). Further evidence for this proposed chemical decomposition was obtained from HPLC analyses, which clearly showed the appearance of La@C_{82} in the samples after electrochemical measurements, confirming efficient addend removal during the electron-transfer procedure.

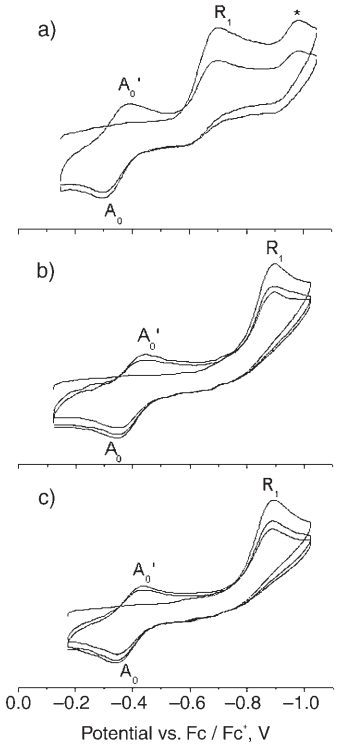

Figure 8. Cyclic voltammograms of a) mono-A, b) mono-B, and c) mono-C in o-dichlorobenzene (0.1 M (nBu)$_4$NPF$_6$, 50 mV s^{-1} scan rate).

Mono-E exhibits two reduction waves and one oxidation wave in the range of 0.8 to −2.0 V (Figure 9a). Its first oxidation potential (0.08 V) is almost identical to that of

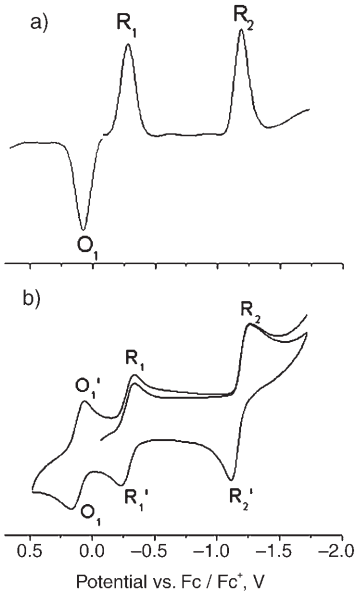

Figure 9. a) Differential pulse and b) cyclic voltammograms of mono-E in o-dichlorobenzene (0.1 M (nBu)$_4$NPF$_6$, 50 and 20 mV s^{-1} scan rate, respectively).

$La@C_{82}$ (0.07 V), while its first reduction potential is shifted positively by 0.14 V relative to the E_1^{red} of $La@C_{82}$, which evidences the strong electron-withdrawing ability of the appended malonate group. Since all the redox waves of mono-E are reversible (Figure 9b), mono-E is expected to be very stable in any of its redox states (cation, anion, and dianion) under argon on the CV timescale. In addition, $[mono\text{-}E]^-$ was prepared by the bulk electrolysis method which was performed at a potential 250 mV more negative than the first reduction potential of mono-E. $[Mono\text{-}E]^-$ is also very stable in air, like $[La@C_{82}]^-$. NMR measurements are therefore practicable for $[mono\text{-}E]^-$.

Conclusion

Herein, we report an unconventional Bingel reaction of $La@C_{82}$. Five monoadducts (mono-A, -B, -C, -D, and -E) have been synthesized and characterized. Among them, mono-A, -B, -C, and -D were revealed to be regioisomers of a singly bonded monoadduct. Mono-E was suggested to be a cycloadduct that is similar to conventional Bingel adducts. Thus, this research has provided another example of an EMF with a distinctly different reactivity to those of empty fullerenes. Furthermore, the thermal stabilities and electrochemical behavior of these monoadducts were investigated. Mono-A, -B, and -C exhibited nearly identical physicochemical properties due to their similar structural features, whereas mono-E possessed different properties, in good agreement with its unique structure. Generally, these studies have not only elucidated the structures and properties of the Bingel monoadducts of $La@C_{82}$, but also provided a synthetic route to novel carboxylated derivatives of EMFs, which are expected to be useful species with biological and medical applications.

Experimental Section

General: All chemicals and solvents were obtained from commercial sources (Wako, Aldrich) and used without further purification unless stated otherwise. Toluene was distilled over sodium/benzophenone. *o*-Dichlorobenzene (ODCB) was distilled over P_2O_5 and stored with molecular sieves.

Synthesis: The reaction of $La@C_{82}$ (4.77 mg, 4.25×10^{-3} mmol) with diethyl bromomalonate (1.8 mg, 7.53×10^{-3} mmol) was conducted at room temperature in the presence of 1,8-diazabicyclo[5.4.0]undec-7-ene (DBU) (0.35 mg, 2.3×10^{-3} mmol) in dry toluene under argon. The reaction proceeded very readily over 2 h. The crude reaction mixture was filtered to remove a small amount of precipitate and separated by multistage separation on HPLC.

HPLC separation: During the multistage HPLC separation procedure, five different columns were used: 5PYE (Nacalai Cosmosil 20×250 mm, toluene as eluent, 9.0 mL min^{-1} flow rate), Buckyprep M (Nacalai Cosmosil 20×250 mm, toluene as eluent, 9.9 mL min^{-1} flow rate), 5PBB (Nacalai Cosmosil 20×250 mm, toluene as eluent, 9.9 mL min^{-1} flow rate), Buckyprep (Nacalai Cosmosil 20×250 mm, toluene as eluent, 9.0 mL min^{-1} flow rate), and Buckyclutcher [Nacalai Cosmosil 20×500 mm, toluene and hexane (3:1) as eluent, 9.9 mL min^{-1} flow rate].

ESR spectroscopy: ESR spectra of mono-A, -B, -C, -E, as well as the mixture of mono-B and -D, were recorded with a Bruker ESR 300E spectrometer. Before measurements were taken, all samples in toluene were degassed and sealed in ESR tubes.

NMR spectroscopy: For the NMR measurements, samples of mono-A, -C, and the mixture of mono-B and -D were dissolved in $CDCl_3/CS_2$ (ca. 1:1). The anion of mono-E was dissolved in $[D_6]$acetone/CS_2 (4:1). ^{13}C NMR spectra were recorded at 125 MHz with a Bruker DRX 500 spectrometer with a CryoProbe system. $[Cr(acac)_3]$ and TMS were used as a relaxant and reference ($\delta=0.00$ ppm), respectively. ^1H NMR spectra were recorded at 500 MHz with the same spectrometer.

UV/Vis/NIR spectroscopy: UV/Vis/NIR spectra of mono-A, B, C, and E in toluene were recorded with a Shimadzu UV-3150 spectrometer using a quartz cell and 1-nm resolution.

Mass spectrometry: Matrix-assisted laser desorption-ionization time-of-flight (MALDI-TOF) mass spectra of mono-A, -B, -C, and -E, as well as the mixture of mono-B and D, were recorded with a Bruker BIFEX-III mass spectrometer using 1,1,4,4-tetraphenyl-1,3-butadiene as the matrix. The measurements were performed in both positive and negative ion modes.

Electrochemical measurements: Differential pulse voltammetry (DPV), cyclic voltammetry (CV), and controlled-potential bulk electrolyses in ODCB were carried out using a BAS CW-50 instrument. A conventional three-electrode cell consisting of a platinum working electrode, a platinum counter-electrode, and a saturated calomel reference electrode (SCE) was used for CV and DPV measurements. $(n\text{Bu})_4NPF_6$ was used as the supporting electrolyte. All potentials were recorded against a SCE reference electrode and corrected against Fc/Fc^+. DPV and CV were measured at a scan rate of 20 and 50 mV s^{-1}, respectively.

Controlled-potential bulk electrolysis (CPE) was performed using an H-type cell with two platinum gauze electrodes as the working and counter-electrodes, respectively. $[Mono\text{-}E]^-$ was obtained under argon in ODCB containing 0.1 M $(n\text{Bu})_4NClO_4$ by setting the applied potential at a value 250 mV more negative than the $E_{1/2}$ value of the $[mono\text{-}E]^-$/mono-E redox couple. The freshly prepared $[mono\text{-}E]^-$ was then transferred from the bulk cell to a 1.00 cm quartz cuvette under argon to measure its UV/Vis/NIR spectrum. The excess supporting electrolyte was precipitated from the solvent by adding carbon disulfide to ODCB and then removed by filtration. The solvent was evaporated under reduced pressure. The residual brown solid was washed by hexane and dissolved in $[D_6]$acetone/CS_2 (4:1) for NMR analysis.

Mono-A: ^1H NMR (500 MHz, $CDCl_3/CS_2$): $\delta=4.50$–4.60 (m, 4H; OCH_2CH_3), 1.50 (t, $J=7$ Hz, 3H; OCH_2CH_3), 1.48 ppm (t, $J=7$ Hz, 3H; OCH_2CH_3); ^{13}C NMR (125 MHz, $CDCl_3/CS_2$): $\delta=164.91$ ($CO_2C_2H_5$), 164.71 ($CO_2C_2H_5$), 157.27, 156.62, 156.30, 152.33, 150.33, 149.65, 149.48, 149.21, 148.80, 148.61, 148.15, 148.00, 147.55, 147.42, 146.93, 146.32, 145.53, 145.45, 145.32, 144.37, 144.05 (two overlapping signals), 144.02, 143.92, 143.83, 143.78, 143.66, 143.29, 143.21, 143.15, 142.70, 142.68, 142.53, 142.25, 141.87, 141.72, 141.07, 140.84, 140.56, 140.26, 140.23, 140.13, 139.98, 139.92, 138.91, 138.86, 138.74, 138.65, 138.57, 138.44, 138.15, 137.93, 137.79, 137.72, 137.68, 136.91, 136.87, 136.78, 136.58, 136.37, 136.26, 135.90, 135.85, 135.47, 135.40, 135.17 (two overlapping signals), 134.78, 134.56, 134.34, 134.25, 134.22, 133.84, 133.77, 133.36, 132.64, 132.52, 131.69, 130.97, 130.44, 130.36, 69.42 ($CBr(CO_2C_2H_5)_2$), 63.99 (OCH_2CH_3), 63.71 (OCH_2CH_3), 60.46 (fullerenyl sp^3 carbon), 14.16 (OCH_2CH_3), 14.13 ppm (OCH_2CH_3); MS (MALDI-TOF): *m*/*z*: calcd for $LaC_{89}H_{10}O_4$ ($[M-Br]^+$): 1280.96, LaC_{82}: 1122.89; found: 1281.57, 1123.39.

Mono-B: ^1H NMR (500 MHz, $CDCl_3/CS_2$): $\delta=4.60$–4.69 (m, 4H; OCH_2CH_3), 1.53 (t, $J=7$ Hz, 3H; OCH_2CH_3), 1.52 ppm (t, $J=7$ Hz, 3H; OCH_2CH_3); ^{13}C NMR (125 MHz, $CDCl_3/CS_2$): $\delta=178.08$, 169.47, 165.14 ($CO_2C_2H_5$), 164.91 ($CO_2C_2H_5$), 161.56, 160.81, 151.64, 149.70, 148.79, 148.67, 148.52, 148.06, 147.89, 147.45, 147.16, 146.97, 146.84, 146.79, 146.29, 146.19, 146.08, 146.00, 145.86, 145.60, 144.49, 144.46, 143.64, 143.55, 143.28, 143.11, 143.09, 143.02, 142.89, 142.59, 142.56 (two overlapping signals), 142.40, 142.07, 141.74, 141.67, 141.50, 141.45, 141.18, 140.28, 140.20, 139.85, 139.69, 139.23, 139.01, 138.99, 138.80, 138.73, 138.60, 138.50, 137.73, 137.70, 137.67, 137.61 (two overlapping signals), 137.49, 137.00, 136.44, 136.30, 136.26, 136.20, 136.09, 136.00, 135.71 (two overlap-

ping signals), 135.42, 135.02, 134.95, 134.43, 134.41, 134.38, 134.15, 133.71 (two overlapping signals), 133.37, 131.99, 131.83, 129.81, 129.25, 68.51 (CBr(CO_2Et)$_2$), 64.11 (OCH_2CH$_3$), 63.92 (OCH_2CH$_3$), 61.10 (fullerenyl sp^3 carbon), 14.22 (OCH$_2$$CH_3$), 14.16 ppm (OCH$_2$$CH_3$); MS (MALDI-TOF, positive): m/z: calcd for $LaC_{89}H_{10}O_4$ ([M−Br]$^+$): 1280.96, LaC_{82}: 1122.89; found: 1280.80, 1122.79.

Mono-C: ^{1}H NMR (500 MHz, $CDCl_3/CS_2$): δ = 4.50–4.60 (m, 4H; OCH_2CH$_3$), 1.42 (t, J = 7 Hz, 3H; OCH$_2$$CH_3$), 1.40 ppm (t, J = 7 Hz, 3H; OCH$_2$$CH_3$); ^{13}C NMR (125 MHz, $CDCl_3/CS_2$): δ = 175.39, 165.05 (2C; CO$_2$C$_2$H$_5$), 164.80, 158.38, 152.53, 150.33, 149.63, 149.35, 148.94, 148.66, 147.60, 147.42, 147.39, 146.99, 146.90, 146.86, 146.77, 146.70, 146.54, 145.40 (three overlapping signals), 144.84, 144.55, 144.52, 143.88, 143.70, 143.47, 143.30, 143.21, 143.01, 142.98, 142.80, 142.10, 142.08, 141.90, 141.84, 141.48, 141.44, 141.29, 141.09, 140.91, 140.59, 140.49, 140.36, 140.16, 139.78, 139.56, 138.90, 138.79, 138.03, 138.00, 137.77, 137.50, 137.31, 137.27, 137.23, 137.18, 137.09, 136.82, 136.34, 135.74, 135.49, 135.27, 135.23, 135.09, 134.95, 134.76, 134.41, 134.15, 133.61 (two overlapping signals), 133.48, 133.30, 133.25, 133.12, 133.04, 131.63, 131.21, 131.05, 130.26, 129.41, 69.32 (CBr(CO$_2$C$_2$H$_5$)$_2$), 64.09 (OCH_2CH$_3$), 64.04 (OCH_2CH$_3$), 63.70 (fullerenyl sp^3 carbon), 14.07 (OCH$_2$$CH_3$), 14.03 ppm (OCH$_2$$CH_3$); MS (MALDI-TOF): m/z: calcd for $LaC_{89}H_{10}O_4$ ([M−Br]$^+$): 1280.96, LaC_{82}: 1122.89; found: 1280.97, 1122.91.

Mono-D: ^{1}H NMR (500 MHz, $CDCl_3/CS_2$): δ = 4.35–4.43 (m, 4H; OCH_2CH$_3$), 1.37 (t, J = 7 Hz, 3H; OCH$_2$$CH_3$), 1.33 ppm (t, J = 7 Hz, 3H; OCH$_2$$CH_3$); ^{13}C NMR (125 MHz, $CDCl_3/CS_2$): δ = 169.54, 164.33 (CO$_2$C$_2$H$_5$), 164.16 (CO$_2$C$_2$H$_5$), 163.99, 161.22 157.33, 156.72, 156.38, 155.03, 154.14, 153.34, 153.06, 152.39, 151.88, 151.36, 150.73, 150.13, 149.40, 149.10, 148.59, 148.49, 147.63, 146.36, 145.82, 145.78, 145.65, 145.50, 145.49, 145.40, 145.22, 145.16, 145.14, 145.01, 144.29, 144.27, 144.09, 143.97, 143.91, 143.85, 143.74, 143.72, 142.84, 142.35, 141.59, 141.24, 140.53, 140.31 (two overlapping signals), 139.63, 139.52, 139.25, 139.12 (two overlapping signals), 138.57, 138.18, 138.01, 137.25, 137.09, 136.89, 136.83, 136.66 (three overlapping signals), 136.50, 136.36, 135.95, 135.82, 135.29, 134.84, 134.74, 134.05 (two overlapping signals), 133.81, 133.61, 133.51, 133.23, 131.90, 131.17, 131.08, 128.92, 128.22, 128.14, 127.58, 67.84 (CBr(CO$_2$C$_2$H$_5$)$_2$), 63.72 (OCH_2CH$_3$), 63.64 (OCH_2CH$_3$), 57.02 (fullerenyl sp^3 carbon), 13.98 (OCH$_2$$CH_3$), 13.94 ppm (OCH$_2$$CH_3$).

Mono-E: The NMR data were obtained from [Mono-E]$^-$. ^{1}H NMR (500 MHz, [D$_6$]acetone/CS_2): δ = 4.19–4.24 (m, 4H; OCH_2CH$_3$), 1.23 (t, J = 7 Hz, 3H; OCH$_2$$CH_3$), 1.21 ppm (t, J = 7 Hz, 3H; OCH$_2$$CH_3$); ^{13}C NMR (125 MHz, [D$_6$]acetone/CS_2): δ = 165.92 (CO$_2$C$_2$H$_5$), 165.84 (CO$_2$C$_2$H$_5$), 158.31, 156.50, 156.40, 153.88, 151.92, 151.89, 151.69, 151.65, 151.52, 151.47, 150.86, 150.79, 150.34, 149.81, 149.22, 149.03, 148.27, 148.09, 147.98, 147.45, 147.34, 146.30, 146.27, 145.99, 145.76, 145.03, 144.69, 144.67, 144.54, 144.36 (two overlapping signals), 144.22, 144.17, 144.10, 143.60, 143.14, 143.09, 142.72, 142.57, 142.22, 141.94, 141.40, 141.18, 141.17, 140.51, 140.37, 139.92, 139.61, 139.49, 139.34, 138.82, 138.65, 138.34, 138.27, 138.19, 137.91, 137.68, 137.52, 137.46, 137.31, 137.27, 137.25, 137.01, 136.86, 136.77, 136.75 (two overlapping signals), 136.35, 136.32, 136.23, 135.76, 135.44, 135.34, 134.75, 133.80, 133.52, 130.96, 129.91, 128.34, 118.72, 111.26, 94.52, 65.74 (C(CO$_2$C$_2$H$_5$)$_2$), 63.06 (OCH_2CH$_3$), 63.00 (OCH_2CH$_3$), 14.37 (OCH$_2$$CH_3$), 14.35 ppm (OCH$_2$$CH_3$); MS (MALDI-TOF): m/z: calcd for $LaC_{89}H_{11}O_4$ ([M]$^+$): 1280.96; found: 1281.38.

Acknowledgements

F.L. thanks the Japan Society for the Promotion of Science (JSPS) for a postdoctoral fellowship for a foreigner researcher. This work was supported in part by a Grant-in-aid for the Nanotechnology Supporting Program of the Ministry of Education, Culture, Sports, Science and Technology of Japan.

[1] Y. Chai, T. Guo, C. Jin, R. E. Haufler, L. P. F. Chibante, J. Fure, L. Wang, M. Alford, R. E. Smalley, *J. Phys. Chem.* **1991**, *95*, 7564–7568.

[2] a) S. Nagase, T. Kobayashi, T. Akasaka, T. Wakahara, *Fullerenes: Chemistry, Physics and Technology* (Eds.: K. M. Kadish, R. S. Ruoff), Wiley, New York, **2000**; b) *Endofullerenes: A New Family of Carbon Cluster* (Eds.: T. Akasaka, S. Nagase), Kluwer Academic Publisher, Dordrecht, **2002**.

[3] a) E. Tóth, R. D. Bolskar, A. Borel, G. González, L. Helm, A. E. Merbach, B. Shitaraman, L. J. Wilson, *J. Am. Chem. Soc.* **2005**, *127*, 799–805; b) R. D. Bolskar, A. F. Benedetto, L. O. Hudebo, R. E. Price, E. F. Jackson, S. Wallace, L. J. Wilson, J. M. Alford, *J. Am. Chem. Soc.* **2003**, *125*, 5471–5478; c) M. Okumura, M. Mikawa, T. Yokokawa, Y. Kanazawa, H. Kato, H. Shinohara, *J. Am. Chem. Soc.* **2003**, *125*, 4391–4397; d) H. Kato, Y. Kanazawa, M. Okumura, A. Taninaka, T. Yokokawa, H. Shinohara, *Academic Radiology* **2002**, *9*, S495–S497; e) M. Mikawa, H. Kato, M. Okumura, M. Narazaki, Y. Kanazawa, N. Miwa, H. Shinohara, *Bioconjugate Chem.* **2001**, *12*, 510–514; f) T. P. Thrash, D. W. Cagle, J. M. Alford, K. Wright, G. J. Ehrhardt, S. Mirzadeh, L. J. Wilson, *Chem. Phys. Lett.* **1999**, *308*, 329–336; g) D. S. Bethune, R. D. Johnson, J. R. Salem, M. S. de Vries, C. S. Yannori, *Nature* **1993**, *366*, 123–128.

[4] For Diels–Alder reactions, see: a) E. B. Iezzi, J. C. Duchamp, K. Harich, T. E. Glass, H. M. Lee, M. M. Olmstead, A. L. Balch, H. C. Dorn, *J. Am. Chem. Soc.* **2002**, *124*, 524–525; b) H. M. Lee, M. M. Olmstead, E. Iezzi, J. C. Duchamp, H. C. Dorn, A. L. Balch, *J. Am. Chem. Soc.* **2002**, *124*, 3494–3495; c) X. Lu, J. Xu, X. He, Z. Shi, Z. Gu, *Chem. Mater.* **2004**, *16*, 953–954.

[5] For Prato reactions, see: a) B. Cao, T. Wakahara, Y. Maeda, A. Han, T. Akasaka, T. Kato, K. Kobayashi, S. Nagase, *Chem. Eur. J.* **2004**, *10*, 716–720; b) C. M. Cardona, A. Kitaygorodskiy, A. Ortiz, M. Á. Herranz, L. Echegoyen, *J. Org. Chem.* **2005**, *70*, 5092–5097; c) C. M. Cardona, A. Kitaygorodskiy, L. Echegoyen, *J. Am. Chem. Soc.* **2005**, *127*, 10448–10453.

[6] For carbene addition reactions, see: a) Y. Maeda, Y. Matsunaga, T. Wakahara, S. Takahashi, T. Tsuchiya, M. O. Ishitsuka, T. Hasegawa, T. Akasaka, M. T. H. Liu, K. Kokura, E. Horn, K. Yoza, T. Kato, S. Okubo, K. Kobayashi, S. Nagase, K. Yamamoto, *J. Am. Chem. Soc.* **2004**, *126*, 6858–6859; b) Y. Iiduka, O. Ikenaga, A. Sakuraba, T. Wakahara, T. Tsuchiya, Y. Maeda, T. Nakahodo, T. Akasaka, M. Kako, N. Mizorogi, S. Nagase, *J. Am. Chem. Soc.* **2005**, *127*, 9956–9957; c) Y. Matsunaga, Y. Maeda, T. Wakahara, T. Tsuchiya, M. O. Ishitsuka, N. Mizorogi, K. Kobayashi, S. Nagase, K. M. Kadish, *ITE Lett.*, in press.

[7] a) T. Akasaka, T. Kato, K. Kobayashi, S. Nagase, K. Yamamoto, H. Funasaka, T. Takahashi, *Nature* **1995**, *374*, 600–601; b) L. Feng, X. Zhang, Z. Yu, J. Wang, Z. Gu, *Chem. Mater.* **2002**, *14*, 4021–4022; c) M. Yamada, L. Feng, T. Wakahara, T. Tsuchiya, Y. Maeda, M. Kako, T. Akasaka, T. Kato, K. Kobayashi, S. Nagase, *J. Phys. Chem. A* **2005**, *109*, 6049–6051; d) I. E. Kareev, S. F. Lebedkin, V. P. Bubnov, E. B. Yagubskii, I. N. Ioffe, P. A. Khavrel, I. V. Kuvychko, S. H. Strauss, O. V. Boltalina, *Angew. Chem.* **2005**, *117*, 1880–1883; *Angew. Chem. Int. Ed.* **2005**, *44*, 1846–1849.

[8] R. D. Bolskar, A. F. Benedetto, L. O. Husebo, R. E. Price, E. F. Jackson, S. Wallace, L. J. Wilson, J. M. Alford, *J. Am. Chem. Soc.* **2003**, *125*, 5471–5478.

[9] a) C. Bingel, *Chem. Ber.* **1993**, *126*, 1957–1959; b) A. Hirsch, I. Lamparth, H. R. Karfunkel, *Angew. Chem.* **1994**, *106*, 453–455; *Angew. Chem. Int. Ed. Engl.* **1994**, *33*, 437–438; c) A. Hirsch, I. Lamparth, T. Grösser, H. R. Karfunkel, *J. Am. Chem. Soc.* **1994**, *116*, 9385–9386.

[10] a) Y. Kubozono, H. Maeda, Y. Takabayashi, K. Hiraoka, T. Nakai, S. Kashino, S. Emura, S. Ukita, T. Sogabe, *J. Am. Chem. Soc.* **1996**, *118*, 6998–6999; b) S. P. Solodovnikov, B. L. Tumanskii, V. V. Bashilov, S. F. Lebedkin, V. I. Skolov, *Russ. Chem. Bull.* **2001**, *110*, 2242–2244; c) S. P. Solodovnikov, S. F. Lebedkin, *Russ. Chem. Bull.* **2003**, *112*, 1111–1113; d) T. Wakahara, A. Sakuraba, Y. Iiduka, M. Okamura, T. Tsuchiya, Y. Maeda, T. Akasaka, S. Okubo, T. Kato, K. Ko-

bayashi, S. Nagase, K. M. Kadish, *Chem. Phys. Lett.* **2004**, *383–396*, 553–556.
[11] T. Akasaka, T. Wakahara, S. Nagase, K. Kobayashi, M. Waelchli, K. Yamamoto, M. Kondo, S. Shirakura, S. Okubo, Y. Maeda, T. Kato, M. Kako, Y. Nakadaira, R. Nagahata, X. Gao, E. Van Caemelbecke, K. M. Kadish, *J. Am. Chem. Soc.* **2000**, *122*, 9316–9317.
[12] a) L. Feng, T. Nakahodo, T. Wakahara, T. Tsuchiya, Y. Maeda, T. Akasaka, T. Kato, E. Horn, K. Yoza, N. Mizorogi, S. Nagase, *J. Am. Chem. Soc.* **2005**, *127*, 17136–17137.
[13] a) D. S. Bethune, R. D. Johnson, J. R. Salem, M. S. De Vries, C. S. Yannoni, *Nature* **1993**, *366*, 123–128; b) K. Kobayashi, S. Nagase, *Chem. Phys. Lett.* **1998**, *282*, 325–329.
[14] R. C. Haddon, *Science* **1993**, *261*, 1545–1550.
[15] T. Suzuki, Y. Maruyama, T. Kato, K. Kikuchi, Y. Achiba, *J. Am. Chem. Soc.* **1993**, *115*, 11006–11007.
[16] T. Wakahara, A. Han, Y. Niino, Y. Maeda, T. Akasaka, T. Suzuki, K. Yamamoto, M. Kako, Y. Nakadaira, K. Kobayashi, S. Nagase, *J. Mater. Chem.* **2002**, *12*, 2061–2064.
[17] In the EC mechanism an electron-transfer step (E) is followed by a chemical reaction (C), see: R. Kessinger, J. Crassous, A. Herrmann, M. Rüttimann, L. Echegoyen, F. Diederich, *Angew. Chem.* **1998**, *110*, 2022–2025; *Angew. Chem. Int. Ed.* **1998**, *37*, 1919–1922.

Received: December 10, 2005
Published online: April 25, 2006

